

REPORT



Removal of variable domain *N*-linked glycosylation as a means to improve the homogeneity of HIV-1 broadly neutralizing antibodies

Gwo-Yu Chuang, Mangaiarkarasi Asokan, Vera B. Ivleva, Amarendra Pegu , Eun Sung Yang, Baoshan Zhang, Rajoshi Chaudhuri, Hui Geng, Bob C. Lin, Mark K. Louder, Krisha McKee, Sijy O'Dell, Hairong Wang, Tongqing Zhou, Nicole A. Doria-Rose, Lisa A. Kueltz, Q. Paula Lei, John R. Mascola, and Peter D. Kwong 

Vaccine Research Center, National Institute of Allergy and Infectious Diseases, National Institutes of Health, Bethesda, MA, USA

ABSTRACT

Broadly neutralizing antibodies are showing promise in the treatment and prevention of HIV-1, with several now being evaluated clinically. Some lead clinical candidates, including antibodies CAP256-VRC26.25, N6, PGT121, and VRC07-523, have one or more *N*-linked glycosylation sequons in their variable domains (Fvs) from somatic hypermutation, and these glycans increase chemical heterogeneity, complicating the manufacture of these antibodies as products. Here we propose a general method to remove Fv glycans and use this method to develop engineered versions of these four antibodies with Fv glycans removed. When germline residues were introduced to remove each glycan, antibody properties between wild type and mutant were not significantly altered for CAP256-VRC26.25 and PGT121; however, germline mutants for N6 and VRC07-523 showed increased polyreactivity, which is known to correlate with unfavorable *in vivo* pharmacokinetics. To reduce polyreactivity induced by removal of Fv glycan, we mutated aromatic residues and arginines structurally proximal to the removed glycan and identified Fv glycan-removed variants with low polyreactivity for N6 and VRC07-523. Two such variants, N6-N72_LQ-R18_LC_D and VRC07-523-N72_LQ-R24_LC_D, showed thermostability, neutralization potency and breadth, and half-life in humanized FcRn mice that were similar to their wild-type Fv-glycosylated counterparts. The removal of Fv glycan and reduction of chemical heterogeneity were confirmed by liquid chromatography-mass spectrometry. With reduced heterogeneity, the Fv-glycan-removed variants developed here may have utility as products for treating or preventing infection by HIV-1.

ARTICLE HISTORY

Received 3 June 2020
Revised 28 August 2020
Accepted 11 October 2020

KEYWORDS

Antibody engineering;
broadly neutralizing
antibodies; heterogeneity;
HIV-1; *n*-linked glycosylation;
polyreactivity; structure-
based design

Introduction

HIV-1 broadly neutralizing antibodies have been isolated from chronically infected patients and have promising utility for treatment^{1–9} and prevention of HIV-1 infection.^{10–16} Among the broadly neutralizing antibodies that are undergoing or being planned for clinical trials,¹⁷ CAP256-VRC26.25,¹⁸ N6,¹⁹ PGT121²⁰ and VRC07-523,¹² contained at least one *N*-linked glycosylation sequon in their variable domains (Fvs) acquired through somatic hypermutation (Figure 1a); the presence of such glycan increases the heterogeneity of these antibodies, which reduces their suitability as commercial products.

In this study, we first developed Fv glycan-removed variants for CAP256-VRC26.25, N6, PGT121 and VRC07-523 by reverting the residues involving the Fv *N*-linked glycosylation sequon to the germline amino acid. This approach yielded variants of CAP256-VRC26.25 and PGT121 that preserved antibody properties such as neutralization, polyreactivity, thermostability, and half-life, but substantially increased polyreactivity for N6 and VRC07-523. Both of these antibodies are members of the VRC01 class of broadly neutralizing antibodies, which use heavy chains derived from the VH1-02*02 gene and have neutralization breadths of over 90% with moderate to high potency.^{21–23} We further developed Fv glycan-removed

variants of N6 and VRC07-523 by using a glycan variant that better preserved the chemistry of the site of glycosylation in combination with the alteration of potential polyreactive amino acids proximal to the glycan site. The neutralization and half-life for a subset of these additionally altered Fv-glycan designs were comparable to wild-type antibodies. Moreover, while it has been shown that Fv *N*-linked glycans acquired from somatic hypermutation can contribute to antibody stability,²⁴ we showed that removal of glycans did not result in substantial reduction in antibody thermostability. With reduced glycan heterogeneity, the Fv glycan-removed variants of CAP256-VRC26.25, N6, PGT121 and VRC07-523 developed here can be added to the select panel of HIV-1 antibodies being assessed as products for treating or preventing HIV-1 infection.

Results

Fv-*N*-linked glycan sequons for CAP256-VRC26.25, N6, PGT121 and VRC07-523 are populated with highly diverse glycoforms

To evaluate the glycosylation heterogeneity of the Fv, the glycan profiles were obtained for CAP256-VRC26.25, N6

CONTACT Peter D. Kwong  pdkwong@nih.gov  Vaccine Research Center, National Institute of Allergy and Infectious Diseases, National Institutes of Health, Bethesda, MA 20892, USA

 Supplemental data for this article can be accessed on the [publisher's website](#).

This work was authored as part of the Contributor's official duties as an Employee of the United States Government and is therefore a work of the United States Government. In accordance with 17 U.S.C. 105, no copyright protection is available for such works under U.S. Law.

This is an Open Access article distributed under the terms of the Creative Commons Attribution-NonCommercial License (<http://creativecommons.org/licenses/by-nc/4.0/>), which permits unrestricted non-commercial use, distribution, and reproduction in any medium, provided the original work is properly cited.

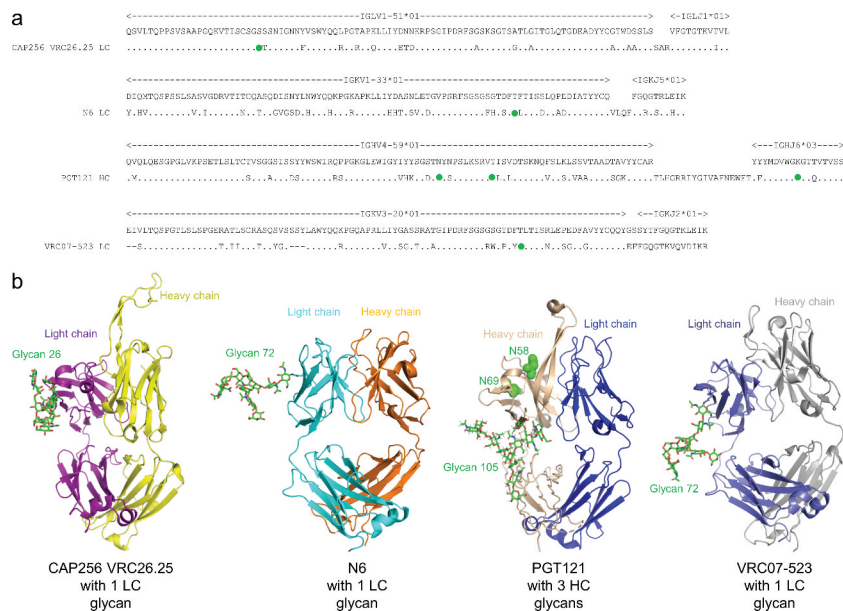


Figure 1. Broadly neutralizing antibodies against HIV-1 generally have substantial somatic mutations and often have Fv *N*-linked glycosylation. (a) Sequences of glycosylated Fv heavy chain (HC) or light chain (LC) for four HIV-1 broadly neutralizing antibodies. Somatic hypermutations are shown, with introduced *N*-linked glycan sequon labeled with green circles. (b) Structures of the four glycosylated antigen-binding fragments (Fabs). Glycans of occupied *N*-linked glycosylation sequon are displayed on structures of PGT121 (PDB:4FQ1), CAP256-VRC26.25 (PDB:5DT1), N6 (PDB:5TE6), and VRC07-523 (modeled from PDB:4OLW) as shown in green sticks, and with the most frequent glycoform being shown (see Table S1). The two *N*-linked glycosylation sequon on PGT121 that were not glycosylated (N58 and N69, see Table S2 and S3) were shown in green spheres.

PGT121, and VRC07-523 using liquid chromatography – mass spectrometry (LC-MS) (Table S1). For CAP256-VRC26.25, the glycan occupancy of light chain N26 was 88%, and the top seven glycoforms were found to contribute to at least 5% of the total peak intensity, respectively. Of the three potential Fv glycosites of PGT121 heavy chain (N58, N68, and N105), only N105 was found to be glycosylated, with the glycan occupancy of heavy chain N105 close to 100% (Table S2-S4). This glycosite displayed a high level of sialylation, and the top six glycoforms were found to contribute to at least 5% of the total peak intensity. With N6 and VRC07-523, the half-life enhancing mutations LS were added to the Fc regions of both antibodies;²⁵ for both N6LS and VRC07-523LS, the glycan occupancy of the light chain site N72 was close to 100%, and high level of sialylation was observed. The top six glycoforms and top four glycoforms were found to contribute to at least 5% of the total peak intensity for N6LS and VRC07-523LS, respectively.

Design of Fv glycan-removed variants for CAP256-VRC26.25, N6, PGT121, and VRC07-523 by germline reversion

CAP256-VRC26.25, N6, PGT121, and VRC07-523 contained *N*-linked glycosylation sites in the Fv region, all obtained from somatic hypermutations (Figure 1a). One *N*-linked glycosylation sequon is present in the light chain Fv of CAP256-VRC26.25, N6, and VRC07-523, while three *N*-linked glycosylation sequons are present in the heavy chain Fv of PGT121 (Figure 1b).

As a first attempt, we designed Fv glycan-removed variants by reverting the somatic hypermutations that led to the presence of *N*-linked glycosylation sequons in Fv to its germline-

encoding amino acid type. Of the four Fv glycan-removed variants, variants for PGT121 and CAP256-VRC26.25 showed similar levels of polyreactivity compared to their wild-type counterparts, based on HEP-2 cell staining assay (Figure 2a) and anti-cardiolipin ELISA (Figure 2b), while variants for N6 and VRC07-523 (with half-life enhancing mutations LS added²⁵) showed heightened level of polyreactivity. Based on these results, Fv glycan-removed variants for CAP256-VRC26.25 (CAP256-VRC26.25-N26_{LC}S) and PGT121 (PGT121-S60_{HC}N-N68_{HC}T-N105_{HC}K) were further analyzed.

CAP256-VRC26.25-N26_{LC}S and PGT121-S60_{HC}N-N68_{HC}T-N105_{HC}K had similar neutralization potency and half-life but substantially reduced heterogeneity compared to their wild-type counterparts

To determine if other antibody properties had been altered by the removal of Fv glycans for CAP256-VRC26.25 and PGT121, we evaluated the neutralization and half-life of CAP256-VRC26.25-N26_{LC}S and PGT121-S60_{HC}N-N68_{HC}T-N105_{HC}K. Both CAP256-VRC26.25-N26_{LC}S and PGT121-S60_{HC}N-N68_{HC}T-N105_{HC}K displayed a similar neutralization potency and breadth to their respective wild-type counterparts when assessed with a 9-strain virus panel (Figures 3a and 4a). We also compared pharmacokinetics of the CAP256-VRC26.25-N26_{LC}S and PGT121-S60_{HC}N-N68_{HC}T-N105_{HC}K to their respective wild-type counterparts in human FcRn transgenic mice and observed that they have similar half-life (Figures 3b and 4b). Finally, we showed that the Fv glycans and its associated heterogeneity at the light chain residue were completely removed from CAP256-VRC26.25-N26_{LC}S and PGT121-S60_{HC}N-N68_{HC}T-N105_{HC}K based on LC-MS data (Figures 3c and 4c, Table S4).

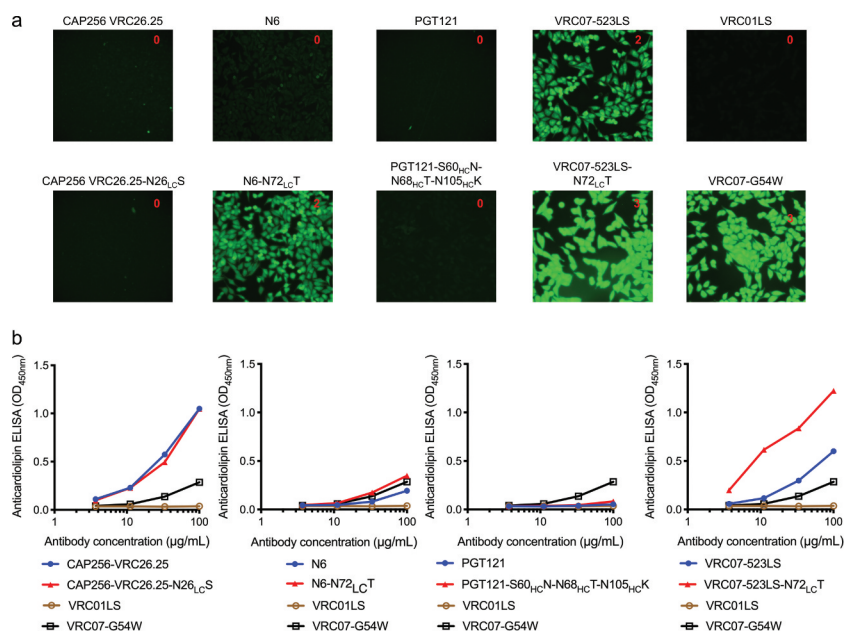


Figure 2. Polyreactivity of N6 and VRC07-523LS is enhanced by reversion of somatic mutation, N72_{LC}T, which removes the introduced N-linked glycan. (a) HEP-2 cell staining (antibody concentration: 25 µg/ml) and (b) anticardiolipin ELISA for CAP256-VRC26.25, N6, PGT121, VRC07-523LS, and their glycan knockouts based on germline encoding residues. For CAP256-VRC26.25 and PGT121 there was no observable difference between wild type and glycan knockouts in both assays, while for N6 and VRC07-523LS higher polyreactivity for the glycan knockout was observed.

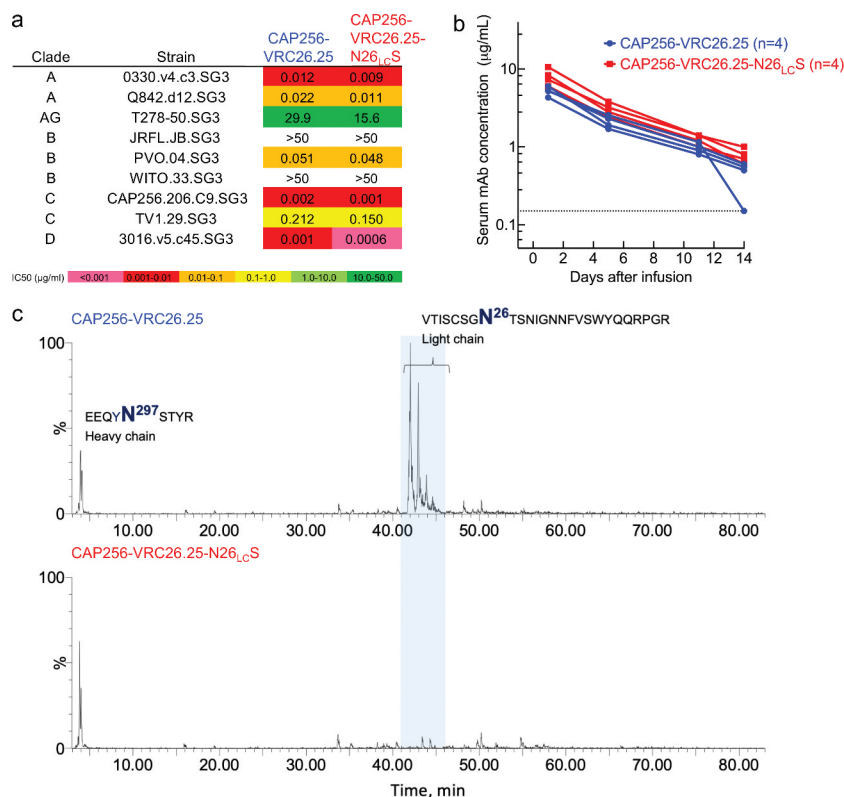


Figure 3. Neutralization, thermostability, pharmacokinetics, and heterogeneity of CAP256-VRC26.25-N26_{LC}S. (a) Neutralization IC₅₀ (µg/ml) of CAP256-VRC26.25 wild type and CAP256-VRC26.25-N26_{LC}S assessed with nine HIV-1 strains. (b) Pharmacokinetic profile for CAP256-VRC26.25 wild type and CAP256-VRC26.25-N26_{LC}S in humanized FcRn mice. Dash line denotes limit of detection. (c) Extracted ion chromatogram (XIC) of [366.137 ± 0.0005] Da corresponding to the signature glycan peak in the tryptic digest of CAP256-VRC26.25 samples: a distribution of the light chain (Fv) glycopeptides in the control material (top trace); only the heavy chain (Fc) glycopeptides are observed in the CAP256-VRC26.25-N26_{LC}S material (bottom trace). XIC peak intensities have been normalized.

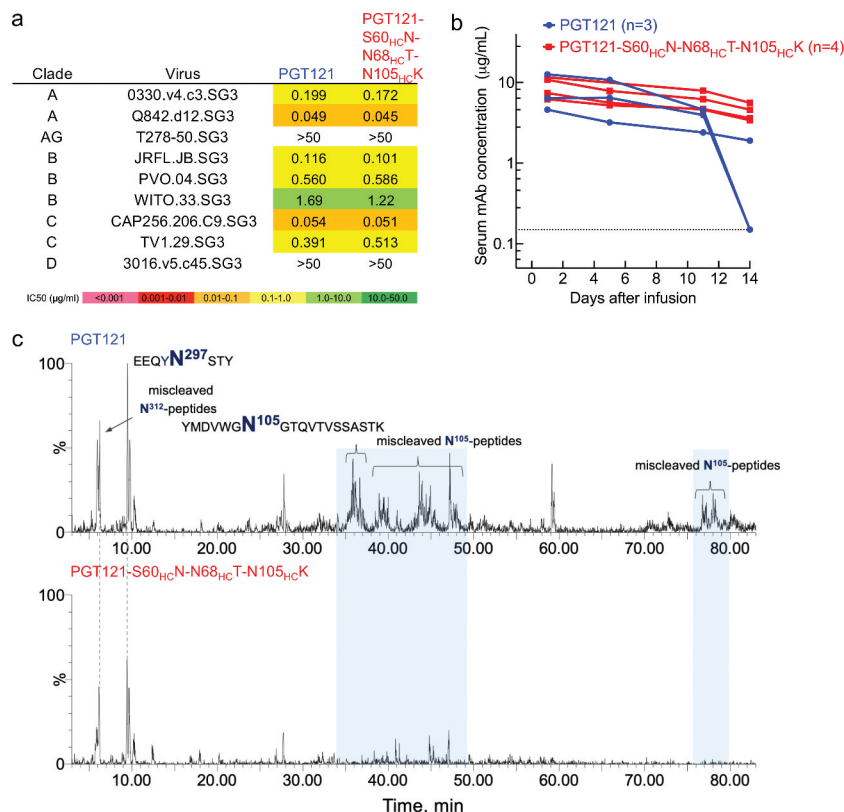


Figure 4. Neutralization, thermostability, pharmacokinetics, and heterogeneity of PGT121-S60_{HC}N-N68_{HT}T-N105_{HC}K. (a) Neutralization IC₅₀ (µg/ml) of PGT121 wild type and PGT121-S60_{HC}N-N68_{HT}T-N105_{HC}K assessed with nine HIV-1 strains. (b) Pharmacokinetic profile for PGT121 and PGT121-S60_{HC}N-N68_{HT}T-N105_{HC}K in humanized FcRn mice. Dash line denotes limit of detection. (c) Extracted ion chromatogram (XIC) of [366.137 ± 0.0005] Da corresponding to the signature glycan peak in the combined [trypsin + chymotrypsin] digests of PGT121 samples: a distribution of the light chain (Fv) glycopeptides in the control material (top trace); only the heavy chain (Fc) glycopeptides are observed in the PGT121-S60_{HC}N-N68_{HT}T-N105_{HC}K material (bottom trace). XIC peak intensities have been normalized.

Presence of native light chain glycan in VRC01-like antibodies

To understand the prevalence of light chain glycan in the VRC01-class antibodies, we searched for *N*-linked glycosylation sequons on germline and mature light chains of representative VRC01-like antibodies from 10 donors (Table 1). Four of the 10 antibodies, VRC01, N6, 3BNC117, and VRC-CH31, had an *N*-linked glycosylation sequon in their framework 3 regions, despite the lack of an *N*-linked glycosylation sequon in the germline light chain for all 10 representative antibodies.

Design of N6 variant with light chain N72 glycan removed and low polyreactivity

An initial attempt to revert N6 N72_{LC} to its germline amino acid, threonine, leads to enhanced polyreactivity. We hypothesized that the light chain glycan might shield polyreactive residues, such as aromatic or arginine residues, which are known to engage lipid.^{26,27} If overlaying glycan were to be removed, then these polyreactive residues might thus need to be altered to maintain an overall low level of polyreactivity (Figure 5). To design such variants of N6, we identified three

Table 1. Analysis of the presence of somatically acquired *N*-linked glycosylation sequon for VRC01-like antibody light chains.

Donor	Antibody	Presence of light chain glycan	Germline gene	Presence of light chain glycan in gl	Specific changes that led to glycosylation	Neutralization breadth (%)
Z258	N6	Yes	IGKV1-33	No	T72N	97.1
NIAID 45	VRC01	Yes	IGKV3-20	No	T72N	90.4
IAVI 57	12A12	No	IGKV1-33	No	N/A	88.9
RU 3	3BNC117	Yes	IGKV1-33	No	T72N	84.6
C38	VRC18	No	IGKV3-20	No	N/A	82.7
CHAVI 0219	VRC-CH31	Yes	IGKV1-33	No	D70N/T72S	80.8
IAVI 74	VRC-PG04	No	IGKV3-20	No	N/A	79.3
IAVI 23	VRC-PG20	No	IGLV2-14	No	N/A	78.4
127/C	VRC23	No	IGKV3-15	No	N/A	63.5
DRV101	DRVIA7	No	IGKV1-5	No	N/A	N/A

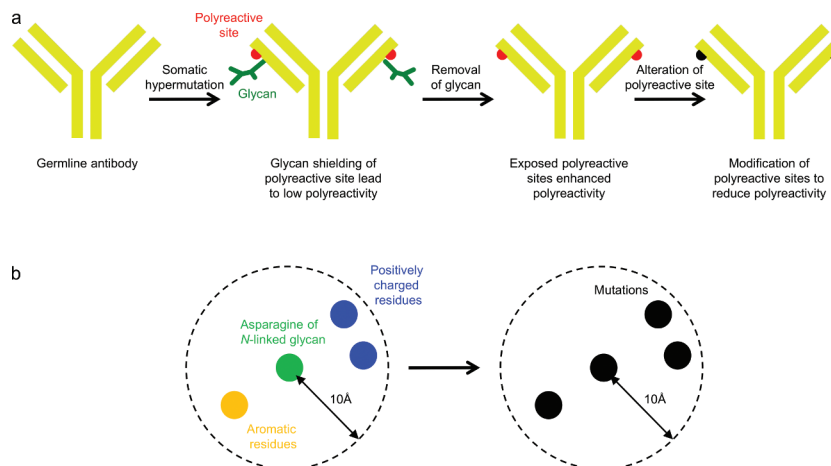


Figure 5. Design of Fv glycan-removed antibodies without enhanced polyreactivity. (a) Schematic of overall approach. (b) Design strategy.

aromatic or arginine residues, R18_{LC}, F67_{LC}, and H68_{LC}, which were proximal to N72_{LC}, and generated variants with mutations at these positions (Figure 6a). To remove the N-linked glycan sequon, we used N72_{LC}Q instead of N72_{LC}T, since glutamine is more similar to asparagine in terms of chemistry, than to the germline-encoded threonine. Based on HEp-2 cell staining and anti-cardiolipin ELISA, N6-N72_{LC}Q showed lower polyreactivity than N6-N72_{LC}T, while two

variants from structure-based design, N6-N72_{LC}Q-R18_{LC}D and N6-N72_{LC}Q-H68_{LC}S, showed even further reduction of polyreactivity, to a level lower than that of wild-type N6 (Figure 6b, 6c, and S1). We evaluated the neutralization of both variants on nine HIV-1 strains and observed them to have comparable neutralization to wild-type N6 (Data S1). In light of these results, we selected N6-N72_{LC}Q-R18_{LC}D, the light chain glycan-removed variant with the lowest polyreactivity,

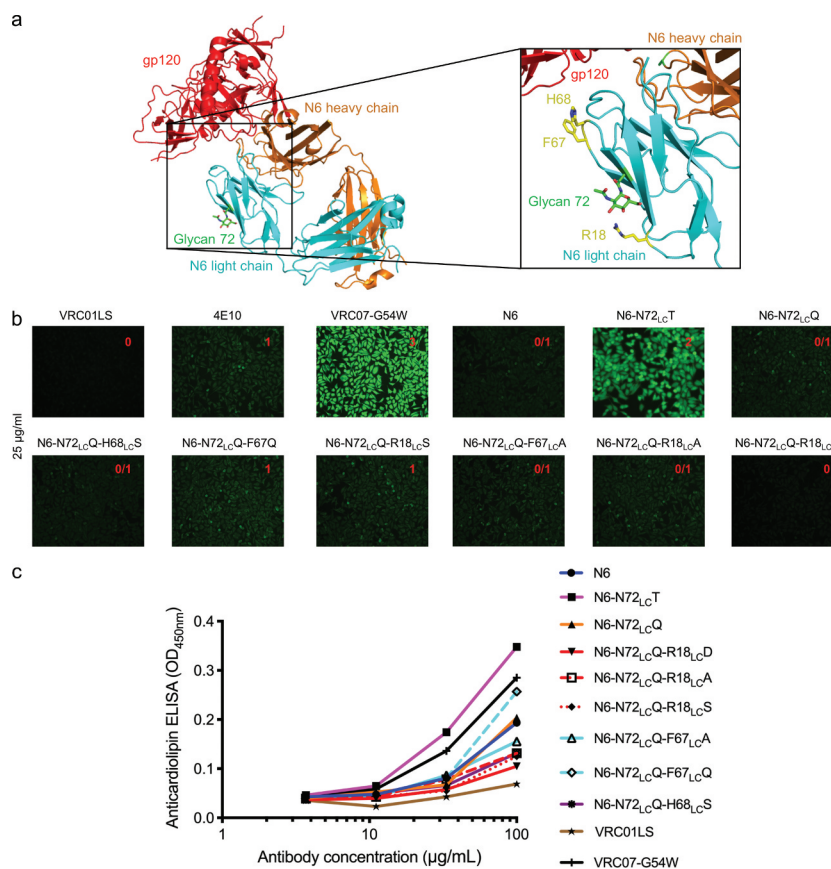


Figure 6. Design of light chain glycan-removed N6 variant. (a) To reduce heightened polyreactivity from removal of light chain glycan 72, mutations were designed to replace aromatic or positively charged residues (shown in yellow) proximal to light chain residue 72 (shown in green). (b) HEp-2 cell staining (antibody concentration: 25 µg/ml) for N6 variants. N6-N72_{LC}Q-R18_{LC}D has similar reactivity as N6 wild type. VRC01LS, 4E10, and VRC07-G54W were used as controls and were assigned to a value between 0 to 3. (c) Anticardiolipin ELISA for N6 variants. N6-N72_{LC}Q-R18_{LC}D showed reduced reactivity as compared to other variants. VRC01LS and VRC07-G54W were used as positive and negative controls, respectively.

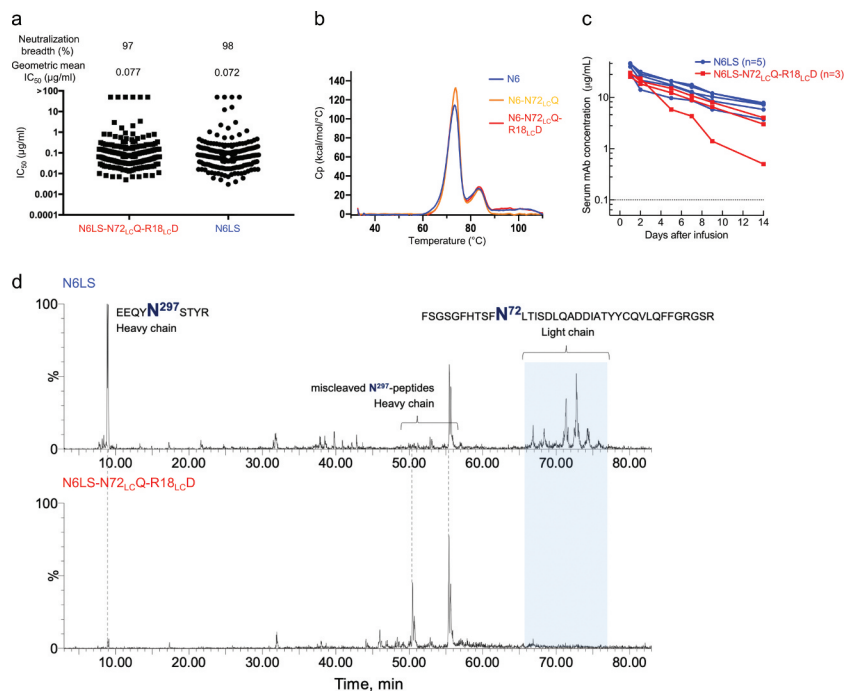


Figure 7. Neutralization, thermostability, pharmacokinetics and heterogeneity of N6-N72_{LC}Q-R18_{LC}D. (a) Neutralization of 208 HIV-1 isolates by N6 wild type and N6-N72_{LC}Q-R18_{LC}D. (b) Differential scanning calorimetry for N6 variants. Removal of glycan did not affect the thermostability of N6. (c) Pharmacokinetic profile for N6LS and N6LS-N72_{LC}Q-R18_{LC}D in humanized FcRn mice. Dash line denotes limit of detection. (d) Extracted ion chromatogram (XIC) of [366.137 ± 0.0005] Da corresponding to the signature glycan peak in the combined [trypsin + LysC] digests of N6LS samples: a distribution of the light chain (Fv) glycopeptides in the control material (top trace); only the heavy chain (Fc) glycopeptides are observed in the N6-N72_{LC}Q-R18_{LC}D-LS material (bottom trace). The XIC peak intensities are normalized.

to assess neutralization with the full 208-strain panel. On this larger cross-clade panel, this variant had comparable neutralization to wild-type N6 (Figure 7a, Data S2), with half-life enhancing mutations LS²⁵ added to both antibodies. We also showed that the removal of the light chain glycan did not affect thermostability (Figure 7b). In addition, we compared *in vivo* pharmacokinetics of the antibodies in human FcRn transgenic mice. N6LS and N6LS-N72_{LC}Q-R18_{LC}D showed similar half-life and rate of clearance (Figure 7c). Finally, we showed the glycan on light chain residue 72 and its associated heterogeneity to be completely removed as assessed by LC-MS (Figure 7d).

Design of VRC07-523LS variant with light chain N72 glycan removed and low polyreactivity

Similar to N6, our initial attempt to remove the Fv glycan by simply reverting VRC07-523LS N72_{LC} to its germline amino acid, threonine, lead to enhanced polyreactivity. As N72_{LC}Q showed lower polyreactivity than N72_{LC}T for N6, we decided to use N72_{LC}Q instead of N72_{LC}T to remove the *N*-linked glycan sequon. To design glycan-removed variants for VRC07-523LS, we identified three arginines, R24_{LC}, R61_{LC}, and R66_{LC}, which were proximal to N72_{LC}, and generated variants with mutations at these positions (Figure 8a). Based on HEp-2 cell staining and anti-cardiolipin ELISA, VRC07-523LS-N72_{LC}Q showed comparable polyreactivity to VRC07-523LS, but the addition of R24_{LC}D or R66_{LC}Q showed substantially reduced polyreactivity, to a level even lower than observed for wild-type VRC07-523LS (Figure 8b, 8c, and S2). We evaluated the neutralization of both variants on nine HIV-1 strains and observed VRC07-523LS-N72_{LC}Q-R24_{LC}D to

have neutralization comparable to VRC07-523LS (Data S1). We evaluated the neutralization of VRC07-523LS-N72_{LC}Q-R24_{LC}D on the full 208-strain panel and found this variant to have comparable neutralization as parent VRC07-523LS (Figure 9a, Data S1). We also showed that the removal of the light chain glycan did not affect thermostability (Figure 9b). In addition, we compared the *in vivo* pharmacokinetics of the antibodies in human FcRn transgenic mice. VRC07-523LS-N72_{LC}Q-R24_{LC}D and VRC07-523LS showed similar half-life and rate of clearance (Figure 9c). Finally, LC-MS revealed the glycan at the light chain residue 72 and its associated heterogeneity to be completely removed (Figure 9d).

Discussion

In this study, we successfully improved the product homogeneity of CAP256-VRC26.25, N6, PGT121, and VRC07-523, four HIV-1 broadly neutralizing antibodies in clinical development, by removing their Fv *N*-linked glycans. The hydrophilic Fv glycans were all acquired during somatic hypermutation, perhaps related to the observation that antibodies generally become less hydrophobic after acquiring somatic hypermutations.²⁸ While simply reverting the *N*-linked glycosylation sequon to their germline counterparts did not affect the other properties of CAP256-VRC26.25 and PGT121, additional engineering steps were required to remove the light chain glycan for N6 and VRC07-523, two of the most potent and broad VRC01-class antibodies, to avoid heightening polyreactivity while maintaining other properties such as neutralization, thermostability, and pharmacokinetics. We found that, while knocking out the light chain *N*-linked glycan

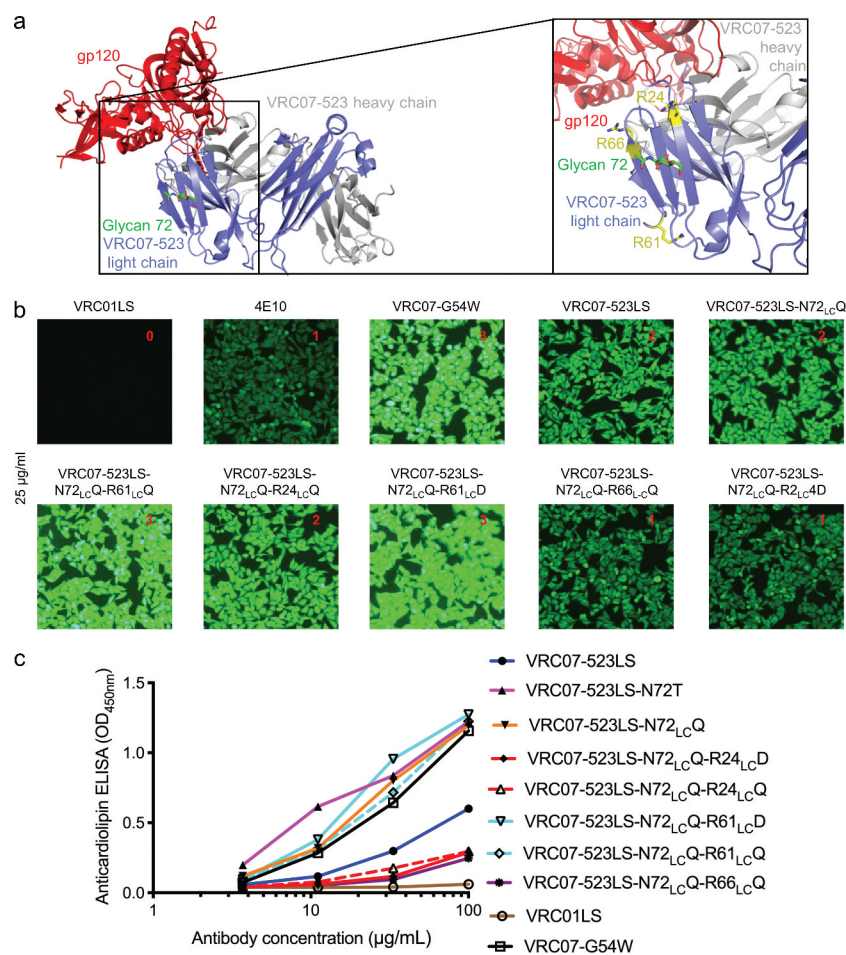


Figure 8. Design of light chain glycan-removed VRC07-523LS variant. (a) To reduce heightened polyreactivity from removal of light chain glycan 72, mutations were designed to replace aromatic or positively charged residues (shown in yellow) proximal to light chain residue 72 (shown in green). (b) HEP-2 cell staining (antibody concentration: 25 µg/ml) for VRC07-523LS variant variants. VRC01LS, 4E10, and VRC07-G54W were used as controls and were assigned to a value between 0 to 3. (c) Anticardiolipin ELISA for VRC07-523LS variants. VRC01LS and VRC07-G54W was used as positive and negative controls, respectively.

sequon increased the polyreactivity of N6 and VRC07-523, low polyreactivity could be recovered by altering glycan-proximal arginines and hydrophobic residues, as these amino acid types have higher membrane-interaction propensity and likely have increased solvent exposure when the proximal *N*-linked glycosylation is removed. The method developed here, removing the polyreactive residues proximal to the glycosylation site when germline reversion of the *N*-linked glycosylation sequon enhanced polyreactivity, may have general utility in the removal of somatically acquired Fv glycosylation to improve the homogeneity of antibodies.

This finding is in some aspects the converse of a prior study, in which we reduced polyreactivity by adding *N*-linked glycan proximal to polyreactive residues to shield their interactions with autoantigens.²⁹ Thus, the introduction of *N*-linked glycans can reduce polyreactivity of neighboring residues, and when *N*-linked glycans are removed, this may uncover the polyreactivity of neighboring formerly shielded residues. We note that when knocking out the N72_{LC} glycan for N6, we noticed that replacing the asparagine with a glutamine at this position showed lower polyreactivity than replacing with threonine (Figures 2 and 4), suggesting that the residue to which the glycan is attached should also be tested for its impact on antibody polyreactivity.

The reduced heterogeneity of the polyreactivity-optimized, Fv glycan-removed variants are likely to be beneficial to the manufacturing of CAP256-VRC26.25, N6, PGT121, and VRC07-523. Importantly, we observed no change to the constant region glycan at residue 297, upon removal of the Fv glycan (Table S5). Of note, we observed reduction in expression by up to twofold for the Fv glycan-removed variants, with the lowest-producing variant yielding 50 mg/L from transient transfection. In addition, apparent solubility was reduced by about 30% for the Fv glycan-removed variant for N6 and VRC07-523LS, as assessed by PEG exclusion assay (Figure S3), suggesting that optimization of solution conditions to improve solubility may be required during manufacturing of these variants. It will be interesting to see how the Fv glycan-removed variants obtained in this study fare as clinical products for the prevention and treatment of HIV-1 infection.

Materials and methods

Design of glycan-removed variants

Asparagine to glutamine mutations were used to knockout *N*-linked glycan sequons. To reduce the enhanced

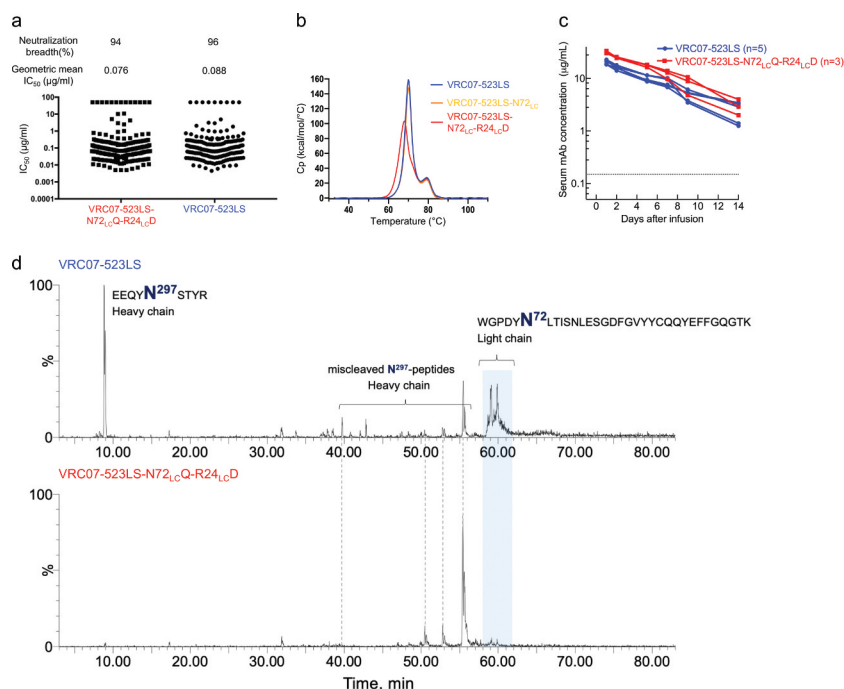


Figure 9. Neutralization, thermostability, pharmacokinetics, and heterogeneity of VRC07-523LS. (a) Neutralization of 10 HIV-1 isolates for VRC07-523LS wild type and VRC07-523LS-N72_{LC}-Q-R24_{LC}-D. (b) Differential scanning calorimetry for VRC07-523LS variants. Removal of glycan did not affect the thermostability of VRC07-523LS. (c) Pharmacokinetic profile for VRC07-523LS and VRC07-523LS-N72_{LC}-Q-R24_{LC}-D in humanized FcRn mice. Dash line denotes limit of detection. (d) Extracted ion chromatogram (XIC) of [366.137 ± 0.0005] Da corresponding to the signature glycan peak in the combined [trypsin + LysC] digests of VRC07-523LS samples: a distribution of the light chain (Fv) glycopeptides in the control material (top trace); only the heavy chain (Fc) glycopeptides are observed in the VRC07-523LS-N72_{LC}-Q-R24_{LC}-D material (bottom trace). XIC peak intensities have been normalized.

polyreactivity stemming from the removal of glycan, we locate all aromatic residues and arginines within 10 Å from the asparagine residue and mutate them to other amino acid types, such as alanine, serine, aspartate, or glutamine.

Antibody expression and purification

Heavy and light chain expression constructs of N6 and VRC07-523 variants were synthesized (Gene Universal Inc., Newark, DE) and cloned into pVRC8400 expression vector. For antibody production, 0.15 mL of Turbo293 transfection reagent (Speed BioSystems) was mixed into 2.5 mL Opti-MEM medium (Life Technology) and incubated for 5 min at room temperature. 50 μg of plasmid DNAs (25 heavy chain and 25 μg of light chain) were mixed into 2.5 mL of Opti-MEM medium in another tube. Then, the diluted Turbo293 were added into Opti-MEM medium containing plasmid DNAs. Transfection reagent and DNA mixture were incubated for 15 min at room temperature, and added to 40 mL of Expi293 cells (Life Technology) at 2.5 million cells/mL. The transfected cells were cultured in shaker incubator at 120 rpm, 37°C, 9% CO₂ for 5 days. At 5 days post-transfection, antibodies in clarified supernatants were purified over 0.5 mL Protein A (GE Health Science) resin in columns. Antibody was eluted with a low pH IgG elution buffer (Pierce), immediately neutralized with one-tenth volume of 1 M Tris-HCL pH 8.0. The antibodies were then buffer exchanged in phosphate-buffered saline (PBS) by dialysis, adjusted concentration to 0.5 mg/mL and filtered (0.22 μm) for neutralization assays.³⁰

Assays to measure polyreactivity

Quanta Lite ACA IgG III ELISA Assay (INOVA Diagnostics, catalog number 708625) was used to test for IgG cardiolipin reactivity per the manufacturer's instructions. Antibodies were tested at dilutions starting at 100 μg/mL and titrated threefold. Here we considered OD (450 nm) values of equal to or greater than threefold of the background ELISA signal as positives. Reactivity to HIV-1 negative human epithelial type 2 (HEp-2) cells was determined by indirect immunofluorescence binding of monoclonal antibodies (mAbs) to HEp-2 cells (ZEUS Scientific, Branchburg, NJ) as described previously.³¹ Briefly, 20 μL of antibody at 25 and 50 μg/mL was placed on a predetermined spot on the surface of an ANA HEp-2 kit slide (Zeus Scientific, catalog number FA2400), incubated for 30 min at room temperature, washed, and developed with 20 μL of ANA HEp-2 conjugate for 30 min. Incubations were performed in humid chambers in the dark. Slides were washed and a drop of mounting agent was placed on each spot prior to the fixing of coverslips. Images were taken on a Nikon Eclipse Ts2R microscope at 25°C in the fluorescein isothiocyanate channel using NIS elements BR4.60.00 software. All images were acquired for 500 ms. Control mAbs were assigned a score between 0 and 3. Test antibodies were assigned scores by visual estimate of fluorescence intensity in comparison to control antibodies.

Virus neutralization

Single-round-of-replication Env pseudoviruses were prepared, titers were determined, and the pseudoviruses were used to

infect TZM-bl target cells as described previously in an optimized and qualified automated 384-well format.³² Briefly, antibodies were serially diluted, a constant amount of pseudovirus added, and plates incubated for 60 minutes; followed by addition of TZM-bl cells which express luciferase upon viral infection. The plates were incubated for 48 hours and then lysed, and luciferase activity was measured. Percent neutralization was determined by the equation: (virus only)-(virus+antibody)/(virus only) multiplied by 100. Data are expressed as the antibody concentration required to achieve 50% neutralization (IC₅₀) and calculated using a dose-response curve fit with a 5-parameter nonlinear function. We used a previously described panel^{21,33,34} of 208 geographically and genetically diverse Env pseudoviruses representing the major subtypes and circulating recombinant forms. The IC₅₀ values reported here are from the complete set of 208 viruses run at the Vaccine Research Center.

Differential scanning calorimetry

A high-precision differential scanning VP-DSC microcalorimeter (GE Healthcare/MicroCal) was used to measure the heat capacity of the trimers. In brief, samples were diluted to 0.3 mg/mL with PBS. Thermal denaturation scans were performed from 30°C to 110°C at a rate of 1°C/min.

Pharmacokinetic study in human neonatal Fc receptor (FcRn) transgenic mice

Human FcRn transgenic mice (FcRn^{-/-} hFcRn (32) Tg mice, JAX stock #014565, The Jackson Laboratory)^{35,36} were used to assess the pharmacokinetics of wild type and Fv glycan-removed antibodies. Each animal was infused intravenously with 5 mg mAb/kg of body weight. Whole blood samples were collected at day 1, 2, 5, 7, 9, 14, 21 and 28. Serum was separated by centrifugation. Serum mAb levels were measured by ELISA using either anti-idiotypic antibodies (for VRC07-523LS; N6LS or N6LS-N72_{LC}Q-R18D; CAP256-VRC26.25 or CAP256-VRC26.25-N26_{LC}S; PGT121 or PGT121-S60_{H₃C}N-N68_{H₃C}T-N105_{H₃C}K) or cognate antigen (resurfaced core 3, RSC3²¹ for VRC07-523LS- N72_{LC}Q- R24_{LC}D) as described previously.¹² All mice were bred and maintained under pathogen-free conditions at an American Association for the Accreditation of Laboratory Animal Care-accredited animal facility at the National Institute of Allergy and Infectious Diseases and housed in accordance with the procedures outlined in the Guide for the Care and Use of Laboratory Animals. All mice were between 6 and 13 weeks of age. The study protocol was evaluated and approved by the National Institutes of Health's Animal Care and Use Committee (ASP VRC-18-747).

Liquid chromatography – mass spectrometry

High purity LC-MS grade water and acetonitrile containing formic acid used for mobile phase preparation, and ammonium bicarbonate reagent were purchased from J.T. Baker (Phillipsburg, NJ). RapiGest™ surfactant was purchased from Waters (Milford, MA). Formic acid was purchased from Pierce

(Rockford, IL). Dithiothreitol (DTT) and iodoacetamide were purchased from ThermoFisher Life Technologies (Grand Island, NY), and Sigma Aldrich (St. Louis, MO), respectively. Trypsin (modified sequencing grade), chymotrypsin, and PNGase F glycosidase were purchased from Promega (Madison, WI).

For the peptide-mapping analysis by LC-MS, the sample concentrations were adjusted to 1.5 mg/mL with 50 mM ammonium bicarbonate, pH 7.4. The mAbs were denatured with RapiGest and reduced with DTT, followed by proteolytic digestions with either trypsin, a combination of [LysC + trypsin], or a combination of [chymotrypsin + trypsin]. The portion of each digest was subsequently deglycosylated with PNGase F for the glycan occupancy study, and another portion was left for monitoring the extent of endogenous or the deamidation possibly induced by the sample preparation.³⁷ All digests were a subject for RPLC separation with MS/MS^E analysis using an Acquity H-Class chromatography system with mass spectrometry detection on a SYNAPT G2 QToF, both from Waters (Milford, MA). The digests were separated on a UPLC Peptide BEH C18 column (300 Å, 1.7 µm, 2.1 mm x 50 mm) (Waters), with the column temperature set to 65°C, at a 0.2 mL/min flow rate; gradient: 0 min – 3%, 1 min – 3%, 91 min – 57%, 91.5 min – 85%, 102 min – 85%, 103 min – 3%, 105 min – 3%. The MS^E elevated-energy channel used linear ramping of the collisional energy from 30 V to 45 V. BiopharmaLynx v. 1.3 was used for the data processing and for the calculation of relative glycosylation; MassLynx v. 4.1 was used for the LC-MS acquisition and for plotting the extracted-ion chromatograms (XICs). The data search included semi-digested and miscleaved peptides, with 10 ppm mass accuracy of the precursor ions and 20 ppm for the fragment ions for initial data scan prior to further data filtering. The XICs of the oxonium ion (366.137 ± 0.0005 Da) were used for the illustration of the overall glycopeptide profiles.

Glycan occupancy was calculated based on the relative amounts of the non-modified and deamidated components resulting from the PNGase F deglycosylation.³⁷ The percentage of each glycoform in the original digest was adjusted for the % occupancy in the corresponding deglycosylated proteolytic digests. The amount of deamidated components, together with the XIC profiles, was used for the ultimate proof of the absence of glycosylation at several potential glycosites.

To ensure the legitimate component assignment, a set of verification criteria was applied to filter the automatically processed results: 5 ppm mass accuracy limit for the precursor ion, 15 ppm for the fragment ions, relevant retention time window, and the MS^E-generated characteristic b,y-ion fragments matching the overall spectral quality.

PEG exclusion assay

Stock solutions of CAP256-VRC26.25, CAP256-VRC26.25-N26_{LC}S, PGT121, PGT121-S60_{H₃C}N-N68_{H₃C}T-N105_{H₃C}K, N6 and VRC07-523LS were diluted to 1 mg/mL with PBS, pH 7.4 (diluted from 10 X PBS, Biowhittaker, Cat. No. 17–517Q). No dilution was performed on N6-N72_{LC}Q-R18_{LC}D and VRC07-523LS-N72_{LC}Q-R24_{LC}D as the stock concentration was 0.8 mg/mL. Stock solutions of 1X PBS (diluted from 10 X PBS, Biowhittaker, Cat. No. 17–517Q), and 30%

w/v PEG-8,000 (EMD Millipore, Cat. No. 6510) in 1X PBS at pH 7.4 were mixed to prepare various concentrations of PEG solutions ranging from 2.5% to 29.5% (w/v). A volume of 160 μ L (for 1 mg/mL sample) or 150 μ L (for 0.8 mg/mL sample) of each PEG-8,000 solutions was added in triplicate to wells of a 96-well polystyrene plate (Greiner Bio-One, Cat No. 655096) to create a 24-point PEG concentration curve. Forty microliters (40 μ L) of the mAb solution at 1 mg/mL or 50 μ L of the mAb solution at 0.8 mg/mL was then added to each well containing PEG to obtain a final protein concentration of 0.2 mg/mL and PEG concentration ranging from 2% to 22% (w/v).

The plates were sealed using an adhesive film (VWR, Cat No. 60941–120) and incubated overnight at room temperature. Post incubation, the contents of each well were transferred to a 96-well filter plate (Corning, Cat No. 3504) stacked on top of a clear 96 well polystyrene plate (Greiner Bio-One, Cat No. 655096). The plates were then centrifuged at 2465 rcf for 30 min in a swing-bucket centrifuge (Eppendorf 5810 R). The filtrate collected in the bottom clear 96-well polystyrene plate was analyzed on a UV-Visible plate reader (Biotek, Synergy Neo2, Winooski, VT) at 285 nm using PBS as a blank to determine the protein concentration. The protein concentration vs. PEG-8,000 (% w/v) data were plotted using Origin 2016 and were fit to a Hill-slope sigmoidal curve equation to determine the % PEG_{midpoint}.

Acknowledgments

We thank J. Baalwa, D. Ellenberger, F. Gao, B. Hahn, K. Hong, J. Kim, F. McCutchan, D. Montefiori, L. Morris, E. Sanders-Buell, G. Shaw, R. Swanstrom, M. Thomson, S. Tovanabutra, C. Williamson, and L. Zhang for contributing the HIV-1 envelope plasmids used in the 208-strain panel. We thank C. Moore, G. Padilla, S.D. Schmidt, C. Whittaker, and A.B. McDermott for assistance with neutralization assessments on the 208-strain panel. We thank J. Baalwa, D. Ellenberger, D. Gabuzda, F. Gao, B. Hahn, K. Hong, J. Kim, F. McCutchan, D. Montefiori, L. Morris, J. Overbaugh, E. Sanders-Buell, G. Shaw, R. Swanstrom, M. Thomson, S. Tovanabutra, C. Williamson, and L. Zhang for contributing the HIV-1 Envelope plasmids used in our neutralization panel. We thank the Structural Biology Section, Structural Bioinformatics Core, Humoral Immunology Section, and Humoral Immunology Core at the NIH Vaccine Research Center for helpful discussions or comments on the manuscript. This work was supported by the Intramural Research Program of the Vaccine Research Center, NIAID, NIH, the Office of AIDS Research, NIH, and by the Neutralization Antibody Consortium of the International AIDS Vaccine Initiative (IAVI).

Abbreviations

FcRn
neonatal Fc receptor

Fv
variable domain

HEp-2
human epithelial type 2

LC-MS
liquid chromatography – mass spectrometry

mAbs
monoclonal antibodies

PBS
phosphate-buffered saline

XIC
extracted-ion chromatogram

Disclosure of Potential Conflicts of Interest

No potential conflicts of interest were disclosed.

Funding

This work was supported by the Intramural Research Program of the Vaccine Research Center, National Institute of Allergy and Infectious Diseases, National Institutes of Health [ZIA AI005022-20].

ORCID

Amarendra Pegu  <http://orcid.org/0000-0003-3564-6453>
Peter D. Kwong  <http://orcid.org/0000-0003-3560-232X>

References

- Shingai M, Nishimura Y, Klein F, Mouquet H, Donau OK, Plishka R, Buckler-White A, Seaman M, Piatak M Jr., Lifson JD, et al. Antibody-mediated immunotherapy of macaques chronically infected with SHIV suppresses viraemia. *Nature*. 2013;503(7475):277–80. doi:10.1038/nature12746.
- Barouch DH, Whitney JB, Moldt B, Klein F, Oliveira TY, Liu J, Stephenson KE, Chang HW, Shekhar K, Gupta S, et al. Therapeutic efficacy of potent neutralizing HIV-1-specific monoclonal antibodies in SHIV-infected rhesus monkeys. *Nature*. 2013;503(7475):224–28. doi:10.1038/nature12744.
- Julg B, Pegu A, Abbink P, Liu J, Brinkman A, Molloy K, Mojta S, Chandrashekar A, Callow K, Wang K, et al. Virological control by the CD4-binding site antibody N6 in simian-human immunodeficiency virus-infected rhesus monkeys. *J Virol*. 2017;91(16). doi:10.1128/JVI.00498-17
- Horwitz JA, Halper-Stromberg A, Mouquet H, Gitlin AD, Tretiakova A, Eisenreich TR, Malbec M, Gravemann S, Billerbeck E, Dorner M, et al. HIV-1 suppression and durable control by combining single broadly neutralizing antibodies and antiretroviral drugs in humanized mice. *Proc Natl Acad Sci U S A*. 2013;110(41):16538–43. doi:10.1073/pnas.1315295110.
- Bolton DL, Pegu A, Wang K, McGinnis K, Nason M, Foulds K, Letukas V, Schmidt SD, Chen X, Todd JP, et al. Human immunodeficiency virus type 1 monoclonal antibodies suppress acute simian-human immunodeficiency virus viremia and limit seeding of cell-associated viral reservoirs. *J Virol*. 2016;90(3):1321–32. doi:10.1128/JVI.02454-15.
- Lynch RM, Boritz E, Coates EE, DeZure A, Madden P, Costner P, Enama ME, Plummer S, Holman L, Hendel CS, et al. Virologic effects of broadly neutralizing antibody VRC01 administration during chronic HIV-1 infection. *Sci Transl Med*. 2015;7(319):319ra206. doi:10.1126/scitranslmed.aad5752.
- Scheid JF, Horwitz JA, Bar-On Y, Kreider EF, Lu CL, Lorenzi JC, Feldmann A, Braunschweig M, Nogueira L, Oliveira T, et al. HIV-1 antibody 3BNC117 suppresses viral rebound in humans during treatment interruption. *Nature*. 2016;535(7613):556–60. doi:10.1038/nature18929.
- Caskey M, Schoofs T, Gruell H, Settler A, Karagounis T, Kreider EF, Murrell B, Pfeifer N, Nogueira L, Oliveira TY, et al.

- Antibody 10-1074 suppresses viremia in HIV-1-infected individuals. *Nat Med.* 2017;23(2):185–91. doi:10.1038/nm.4268.
9. Caskey M, Klein F, Lorenzi JC, Seaman MS, West AP Jr, Buckley N, Kremer G, Nogueira L, Braunschweig M, Scheid JF, et al. Viraemia suppressed in HIV-1-infected humans by broadly neutralizing antibody 3BNC117. *Nature.* 2015;522(7557):487–91. doi:10.1038/nature14411.
 10. Moldt B, Rakasz EG, Schultz N, Chan-Hui PY, Swiderek K, Weisgrau KL, Piaskowski SM, Bergman Z, Watkins DI, Poignard P, et al. Highly potent HIV-specific antibody neutralization in vitro translates into effective protection against mucosal SHIV challenge in vivo. *Proc Natl Acad Sci U S A.* 2012;109(46):18921–25. doi:10.1073/pnas.1214785109.
 11. Pegu A, Yang ZY, Boyington JC, Wu L, Ko SY, Schmidt SD, McKee K, Kong WP, Shi W, Chen X, et al. Neutralizing antibodies to HIV-1 envelope protect more effectively in vivo than those to the CD4 receptor. *Sci Transl Med.* 2014;6(243):243ra88. doi:10.1126/scitranslmed.3008992.
 12. Rudicell RS, Kwon YD, Ko SY, Pegu A, Louder MK, Georgiev IS, Wu X, Zhu J, Boyington JC, Chen X, et al. Enhanced potency of a broadly neutralizing HIV-1 antibody in vitro improves protection against lentiviral infection in vivo. *J Virol.* 2014;88(21):12669–82. doi:10.1128/JVI.02213-14.
 13. Shingai M, Donau OK, Plishka RJ, Buckler-White A, Mascola JR, Nabel GJ, Nason MC, Montefiori D, Moldt B, Poignard P, et al. Passive transfer of modest titers of potent and broadly neutralizing anti-HIV monoclonal antibodies block SHIV infection in macaques. *J Exp Med.* 2014;211(10):2061–74. doi:10.1084/jem.20132494.
 14. Saunders KO, Pegu A, Georgiev IS, Zeng M, Joyce MG, Yang ZY, Ko SY, Chen X, Schmidt SD, Haase AT, et al. Sustained delivery of a broadly neutralizing antibody in nonhuman primates confers long-term protection against simian/human immunodeficiency virus infection. *J Virol.* 2015;89(11):5895–903. doi:10.1128/JVI.00210-15.
 15. Gautam R, Nishimura Y, Pegu A, Nason MC, Klein F, Gazumyan A, Golijanin J, Buckler-White A, Sadjadpour R, Wang K, et al. A single injection of anti-HIV-1 antibodies protects against repeated SHIV challenges. *Nature.* 2016;533(7601):105–09. doi:10.1038/nature17677.
 16. Moldt B, Le KM, Carnathan DG, Whitney JB, Schultz N, Lewis MG, Borducchi EN, Smith KM, Mackel JJ, Sweat SL, et al. Neutralizing antibody affords comparable protection against vaginal and rectal simian/human immunodeficiency virus challenge in macaques. *AIDS.* 2016;30(10):1543–51. doi:10.1097/QAD.0000000000001102.
 17. Caskey M, Klein F, Nussenzweig MC. Broadly neutralizing anti-HIV-1 monoclonal antibodies in the clinic. *Nat Med.* 2019;25(4):547–53. doi:10.1038/s41591-019-0412-8.
 18. Doria-Rose NA, Bhiman JN, Roark RS, Schramm CA, Gorman J, Chuang GY, Pancera M, Cale EM, Ernandes MJ, Louder MK, et al. New member of the V1V2-directed CAP256-VRC26 lineage that shows increased breadth and exceptional potency. *J Virol.* 2016;90(1):76–91. doi:10.1128/JVI.01791-15.
 19. Huang J, Kang BH, Ishida E, Zhou T, Griesman T, Sheng Z, Wu F, Doria-Rose NA, Zhang B, McKee K, et al. Identification of a CD4-binding-site antibody to HIV that evolved near-pan neutralization breadth. *Immunity.* 2016;45(5):1108–21. doi:10.1016/j.immuni.2016.10.027.
 20. Walker LM, Huber M, Doores KJ, Falkowska E, Pejchal R, Julien JP, Wang SK, Ramos A, Chan-Hui PY, Moyle M, et al. Broad neutralization coverage of HIV by multiple highly potent antibodies [Research Support, N.I.H., Extramural research support, Non-U.S. Gov't Research Support, U.S. Gov't, Non-P.H.S.]. *Nature.* 2011;477(7365):466–70. doi:10.1038/nature10373.
 21. Wu X, Yang ZY, Li Y, Hogerkerp CM, Schief WR, Seaman MS, Zhou T, Schmidt SD, Wu L, Xu L, et al. Rational design of envelope identifies broadly neutralizing human monoclonal antibodies to HIV-1. *Science.* 2010;329(5993):856–61. doi:10.1126/science.1187659.
 22. Zhou T, Zhu J, Wu X, Moquin S, Zhang B, Acharya P, Georgiev IS, Altae-Tran HR, Chuang GY, Joyce MG, et al. Multidonor analysis reveals structural elements, genetic determinants, and maturation pathway for HIV-1 neutralization by VRC01-class antibodies. *Immunity.* 2013;39(2):245–58. doi:10.1016/j.immuni.2013.04.012.
 23. West AP Jr., Diskin R, Nussenzweig MC, Bjorkman PJ. Structural basis for germ-line gene usage of a potent class of antibodies targeting the CD4-binding site of HIV-1 gp120. *Proc Natl Acad Sci U S A.* 2012;109(30):E2083–90. doi:10.1073/pnas.1208984109.
 24. van de Bovenkamp FS, Derksen NIL, van Breemen MJ, de Taeye SW, Ooijevaar-de Heer P, Sanders RW, Rispen T. Variable domain N-linked glycans acquired during antigen-specific immune responses can contribute to immunoglobulin G antibody stability. *Front Immunol.* 2018;9:740. doi:10.3389/fimmu.2018.00740.
 25. Zalevsky J, Chamberlain AK, Horton HM, Karki S, Leung IW, Sproule TJ, Lazar GA, Roopenian DC, Desjarlais JR. Enhanced antibody half-life improves in vivo activity. *Nat Biotechnol.* 2010;28(2):157–59. doi:10.1038/nbt.1601.
 26. Meyers NL, Larsson M, Vorrso E, Olivecrona G, Small DM. Aromatic residues in the C terminus of apolipoprotein C-III mediate lipid binding and LPL inhibition. *J Lipid Res.* 2017;58(5):840–52. doi:10.1194/jlr.M071126.
 27. Li L, Vorobyov I, Allen TW. The different interactions of lysine and arginine side chains with lipid membranes. *J Phys Chem B.* 2013;117(40):11906–20. doi:10.1021/jp405418y.
 28. Shehata L, Maurer DP, Wec AZ, Lilov A, Champney E, Sun T, Archambault K, Burnina I, Lynaugh H, Zhi X, et al. Affinity maturation enhances antibody specificity but compromises conformational stability. *Cell Rep.* 2019;28(13):3300–3308 e4. doi:10.1016/j.celrep.2019.08.056.
 29. Chuang GY, Zhang B, McKee K, O'Dell S, Kwon YD, Zhou T, Blinn J, Lloyd K, Parks R, Von Holle T, et al. Eliminating antibody polyreactivity through addition of N-linked glycosylation. *Protein Sci.* 2015;24(6):1019–30. doi:10.1002/pro.2682.
 30. Kwon Y, Chuang GY, Zhang B, Bailer RT, Doria-Rose NA, Gindin TS. Surface-matrix screening identifies semi-specific interactions that improve potency of a near pan-reactive HIV-1-neutralizing antibody. *Cell Rep.* 2018;22(7):1798–809. doi:10.1016/j.celrep.2018.01.023.
 31. Haynes BF, Fleming J, St Clair EW, Katinger H, Stiegler G, Kunert R, Robinson J, Scarce RM, Plonk K, Staats HF, et al. Cardiophilic polyspecific autoreactivity in two broadly neutralizing HIV-1 antibodies. *Science.* 2005;308(5730):1906–08. doi:10.1126/science.1111781.
 32. Sarzotti-Kelsoe M, Bailer RT, Turk E, Lin CL, Bilaska M, Greene KM, Gao H, Todd CA, Ozaki DA, Seaman MS, et al. Optimization and validation of the TZM-bl assay for standardized assessments of neutralizing antibodies against HIV-1. *J Immunol Methods.* 2014;409:131–46. doi:10.1016/j.jim.2013.11.022.
 33. Georgiev IS, Doria-Rose NA, Zhou T, Kwon YD, Staup RP, Moquin S, Chuang GY, Louder MK, Schmidt SD, Altae-Tran HR, et al. Delineating antibody recognition in polyclonal sera from patterns of HIV-1 isolate neutralization. *Science.* 2013;340(6133):751–56. doi:10.1126/science.1233989.
 34. Cale EM, Gorman J, Radakovich NA, Crooks ET, Osawa K, Tong T, Li J, Nagarajan R, Ozorowski G, Ambrozak DR, et al. Virus-like particles identify an HIV V1V2 apex-binding neutralizing antibody that lacks a protruding loop. *Immunity.* 2017;46(5):777–791 e10. doi:10.1016/j.immuni.2017.04.011.

35. Petkova SB, Akilesh S, Sproule TJ, Christianson GJ, Al Khabbaz H, Brown AC, Presta LG, Meng YG, Roopenian DC. Enhanced half-life of genetically engineered human IgG1 antibodies in a humanized FcRn mouse model: potential application in humorally mediated autoimmune disease. *Int Immunol.* 2006;18(12):1759–69. doi:[10.1093/intimm/dxl110](https://doi.org/10.1093/intimm/dxl110).
36. Roopenian DC, Christianson GJ, Sproule TJ. Human FcRn transgenic mice for pharmacokinetic evaluation of therapeutic antibodies. *Methods Mol Biol.* 2010;602:93–104. doi:[10.1007/978-1-60761-058-8_6](https://doi.org/10.1007/978-1-60761-058-8_6).
37. Ivleva VB, Cooper JW, Arnold FJ, Lei QP. Overcoming challenges in structural characterization of HIV-1 Envelope glycoprotein by LC-MS/MS. *J Am Soc Mass Spectrom.* 2019;30(9):1663–78. doi:[10.1007/s13361-019-02225-3](https://doi.org/10.1007/s13361-019-02225-3).